phys. stat. sol. (b) **215**, 459 (1999)

Subject classification: 63.22.+m; 78.30.Fs; 78.66.Hf; S8.12

Resonant Raman Scattering in Asymmetric Semiconductor Quantum Disks

C. TRALLERO-GINER (a), E. MENÉNDEZ-PROUPIN (a), and S. E. ULLOA (b)

(a) Department of Theoretical Physics, Havana University, Vedado 10400, Havana, Cuba

(b) Department of Physics and Astronomy, and CMSS Program, Ohio University, Athens, Ohio 45701-2979, USA

(Received March 30, 1999)

We report a theoretical study of the first-order resonant Raman scattering by optical phonons in self-assembled quantum dots (SAQDs). We consider the SAQD as a cylindrical disk with elliptical cross section to simulate shape and confinement anisotropies obtained during the SAQD growth. The lateral confinement anisotropy is modelled by harmonic potentials with two different frequencies. In an envelope function Hamiltonian approach and using matrix diagonalization techniques, the exciton wave function and energy states are calculated as function of SAQD parameters. Raman scattering polarizability is obtained for a Fröhlich coupling between exciton and confined-phonons. We analyze how the Raman scattering technique could give information on confinement anisotropy effects and SAQDs geometry. Here, characteristic results for SAQDs of CdSe dots in ZnSe are presented.

1. Introduction

Last few years have seen an explosion in research activities on self-assembled quantum dots (SAQDs) [1]. These structures provide extreme quantum confinement of charge carriers given their nanometer dimensions. Either by photoproduction, doping, or tunneling in a capacitance arrangement [2], electrons and/or holes in these structures experience the strong local potential provided by structural constraints, as well as by long-ranged strain fields. The effective confinement potential then includes the combined effect of structural as well as lattice and strain anisotropies and may have in general quite a complicated symmetry. Since several growth techniques are employed to fabricate SAQDs, the resulting geometries and sample configurations yield a variety of different structures [1]. Structural geometries vary from faceted pyramids [3] to smoother lenticular shapes [1], depending critically on growth and local environment conditions. Photoluminescence (PL) and PL excitation (PLE) experiments are routinely used to provide information on the overall size of the resulting SAQDs, since due to the carrier confinement there is a strong correlation between decreasing sizes and the larger blue-shifting of the PL signal. Mapping of the quantum dot shape is also accomplished by a variety of microscopy techniques, from TEM to AFM, but quantitative and detailed information on the effective potential in a given structure is difficult to obtain.

In this paper, we present a theoretical treatment of the resonant Raman scattering by confined phonons in SAQDs. By analysis of the elements entering these experiments, namely the effects of the effective potential on excitonic states, the general case of LO-phonon dispersion for modes confined in the dot, and a detailed calculation of the various matrix elements involved in the Fröhlich coupling, we provide the basis for

quantitative analysis of Raman experiments in these systems. For concreteness, we focus our attention here on a model of asymmetric dot confinement, where the effective potential is assumed to be that of a cylindrical pill-box with elliptical cross section, and we study the effects of this non-circular geometry on the Raman scattering process efficiency. We find that the asymmetry indeed has strong and clear signatures in the light scattering. Moreover, detailed analysis of the Raman coupling could give information on the effective mass of the carriers.

2. Resonant Raman Scattering in Quantum Disks

The resonant Raman polarizability is related to the microscopic amplitude through the expression [4]

$$a = \frac{\eta_{\rm l}\eta_{\rm s}}{2\pi}\,\frac{V_{\rm c}}{u_0}\,\frac{1}{\hbar\omega_{\rm l}}\sum_{\mu_1,\mu_2}\frac{\langle f|\,H_{\rm E-R}\,|\mu_2\rangle\,\langle\mu_2|\,H_{\rm E-L}\,|\mu_1\rangle\,\langle\mu_1|\,H_{\rm E-R}\,|i\rangle}{(\hbar\omega_{\rm s}-E_{\mu_2}+i\Gamma_{\mu_2})\,(\hbar\omega_{\rm l}-E_{\mu_1}+i\Gamma_{\mu_1})}\,, \tag{1}$$

where η is the refractive index, $\omega_{\rm l}(\omega_{\rm s})$ is the incoming(outgoing) light frequency, u_0 is the relative displacement, and $V_{\rm c}$ is the volume of the primitive cell. The kets $|\mu_1\rangle$ and $|\mu_2\rangle$ refer to the excitonic intermediate states in the QD, E_μ and Γ_μ are their respective energies and lifetime broadenings, and $H_{\rm E-R}$ and $H_{\rm E-L}$ are the exciton–radiation and the exciton–lattice interaction Hamiltonians, respectively. The exciton–radiation coupling constant in the dipole approximation is proportional to [5] $\int \Psi_\mu(\mathbf{r}_{\rm e}=\mathbf{r}_0,\mathbf{r}_{\rm h}=\mathbf{r}_0)\,{\rm d}^3r_0$, where $\Psi_\mu(\mathbf{r}_{\rm e},\mathbf{r}_{\rm h})$ is the exciton wave function. In the following we consider the QD grown along the [001] direction denoted by z, and its geometry modeled as a quantum disk. It is assumed that the quantum disk lengths L_x, L_y are larger than L_z and the LO-phonons are confined along the z-direction with eigenfrequencies $\omega_n^2=\omega_{\rm L}^2-\beta_{\rm L}^2(n\pi/L_z)^2; n=1,2,\ldots$ [7], where $\omega_{\rm L}$ and $\beta_{\rm L}$ describe the bulk LO-phonon dispersion. In nanostructure semiconductors, such as quantum wells and QDs and in the backscattering configuration $z(x,x)\,\bar{z}$, with x parallel to [100] direction, the Fröhlich mechanism becomes the stronger coupling for light frequencies in resonance with the excitonic states [6]. The exciton–LO-phonon coupling constant in the dipole approximation for the in-plane phonon wavevector is given by [7] $S_{\mu_1}^{\mu_2}=\langle\mu_2|\,\Phi_{\rm F}^{(n)}(z_{\rm e})-\Phi_{\rm F}^{(n)}(z_{\rm h})\,|\mu_1\rangle$ with

$$\Phi_{\rm F}^{(n)}(z)=\frac{C_{\rm F}L_z}{n\pi}\left(\frac{\omega_{\rm L}}{\omega_n}\right)^{1/2}\begin{cases}1-(-1)^n; & z\le-\dfrac{L_z}{2}\,,\\[2mm] 2\cos\left[\dfrac{n\pi}{L_z}\left(z+\dfrac{L_z}{2}\right)\right]; & -\dfrac{L_z}{2}\le z\le\dfrac{L_z}{2}\,,\\[2mm] (-1)^n-1; & z\ge\dfrac{L_z}{2},\end{cases} \tag{2}$$

and $C_{\rm F}$ is the Fröhlich coupling constant. Introducing the above expressions into (1), the Raman polarizability for the Fröhlich-like interaction takes the form

$$a_{\rm F}^{(n)}=\frac{V_{\rm c}}{Vu_0}\,\frac{e^2}{m_0^2\omega_{\rm l}\sqrt{\omega_{\rm l}\omega_{\rm s}}}\sum_{\mu_1,\mu_2}\mathbf{e}_{\rm s}\cdot\mathbf{p}_{\rm vc}\,\frac{\int\Psi_{\mu_2}^*(\mathbf{r},\mathbf{r})\,{\rm d}^3r\int\Psi_{\mu_1}(\mathbf{r},\mathbf{r})\,{\rm d}^3r}{(\hbar\omega_{\rm l}-E_{\mu_1}+i\Gamma_{\mu_1})}\,\mathbf{e}_{\rm l}\cdot\mathbf{p}_{\rm cv}$$
$$\times\left[\frac{\langle\Psi_{\mu_2}|\,\Phi_{\rm F}^{(n)}(z_{\rm e})\,|\Psi_{\mu_1}\rangle-\langle\Psi_{\mu_2}|\,\Phi_{\rm F}^{(n)}(z_{\rm h})\,|\Psi_{\mu_1}\rangle}{(\hbar\omega_{\rm s}-E_{\mu_2}+i\Gamma_{\mu_2})}\right]. \tag{3}$$

For quasi-flat quantum disks, where the condition $L_x, L_y \gg L_z$ is fulfilled, the anisotropy effects along the growth direction can be disregarded. The confining potential in the dot can be assumed, in first approximation, constant. Nevertheless, the asymmetric confinement geometry needs to be taken into account. The excitonic intermediate states are confined into a harmonic potential in the XY plane with frequencies ω_x and ω_y and axes ratio given by $L_x/L_y = \sqrt{\omega_y/\omega_x}$, and a strong confinement regime along the z-axis is assumed. Hence, the exciton problem in the envelope function approximation can be described by a separable Hamiltonian in the XY plane and the Z-motion. The wavefunction is separable into a product of the in-plane wavefunction $\varphi_{N_x,N_y}(\mathbf{R})\,\Theta_m(\boldsymbol{\varrho})$ described by the center-of-mass $\mathbf{R}$ and relative coordinate $\boldsymbol{\varrho}$, and the electron and hole subband wavefunctions $\phi_{n_i}(z_i)$ (i = e, h). The center of mass function φ_{N_x,N_y} corresponds to a two-dimensional harmonic oscillator with quantum numbers N_x, N_y and the m-th state of the relative exciton motion is described in Ref. [8] and given by $\Theta_m(\boldsymbol{\varrho}) = \sum_{n_x,n_y} a_{n_x,n_y}\varphi_{n_x}(x)\,\varphi_{n_y}(y)$. The energies E_m and eigenfunctions Θ_m are obtained by numerical diagonalization techniques from the Hamiltonian describing the 2D exciton relative motion [8]. The total exciton energy is given by $E(m, N_x, N_y, n_e, n_h) = \left(N_x + \frac{1}{2}\right)\hbar\omega_x + \left(N_y + \frac{1}{2}\right)\hbar\omega_y + E_m + E_g + E_{n_e} + E_{n_h}$. As the excitonic Bohr radius is much larger than the electron–hole pair distance mean value along the Z-direction, the three-dimensionality of the Coulomb interaction effect on the exciton binding energy can be treated by perturbation theory of the Hamiltonian $H_p = -e^2/\epsilon\,|\mathbf{r}_e - \mathbf{r}_h| + e^2/\epsilon\,|\boldsymbol{\varrho}_e - \boldsymbol{\varrho}_h|$ ($\boldsymbol{\varrho}$ being the in-plane component of $\mathbf{r}$) [9]. The Raman polarizability a_F for the n-th phonon state is obtained by introducing the calculated matrix elements into Eq. (3). Since the only allowed optical transitions between electron and hole subbands have quantum numbers $n_e - n_h$ equal to an even number, it follows that the Fröhlich interaction is allowed only for phonon states with even quantum number ($n = 2, 4, \ldots$).

3. Results and Discussion

For a SAQD with circular geometry ($\omega_x = \omega_y$, or $L = L_x = L_y$) the states with $N_x + N_y = N$ are all degenerate and according to Eq. (3) the Raman feature will present a sole incoming (or outgoing) resonant peak at laser energy equal to these excitonic transitions, that is $\hbar\omega_l(\hbar\omega_s) = E(m, N_x, N - N_x, n_e, n_h)$. In the case one is dealing with elliptical cross sections, the degeneracy due to the circular symmetry is broken and a set of new incoming and outgoing resonances will appear in the Raman scattering efficiency. The different excitonic transitions of the SAQD can be tuned by the incoming light and their shift in energetic separation give a direct characterization of the quantum disk geometry. As example, we use parameters to describe CdSe SAQD in ZnSe. These islands are grown by molecular beam epitaxy [10,11] or atomic layer epitaxy [11]. In correspondence with bulk phonon data for CdSe ($\omega_L = 209\ \mathrm{cm}^{-1}$) and ZnSe ($\omega_L = 250\ \mathrm{cm}^{-1}$), the CdSe phonons must be confined in the dot. Nevertheless, experimental observation in quantum wells does not present evidence that phonons are confined. The growth conditions and the lattice mismatch stress effect could explain these experimental facts. Due to lack of knowledge on what happens in CdSe/ZnSe quantum disks we prefer to follow the confined model above presented to show the anisotropic geometric influence on Raman scattering. Fig. 1 shows the $|a_F^{(n)}|^2$ Raman polarizability as

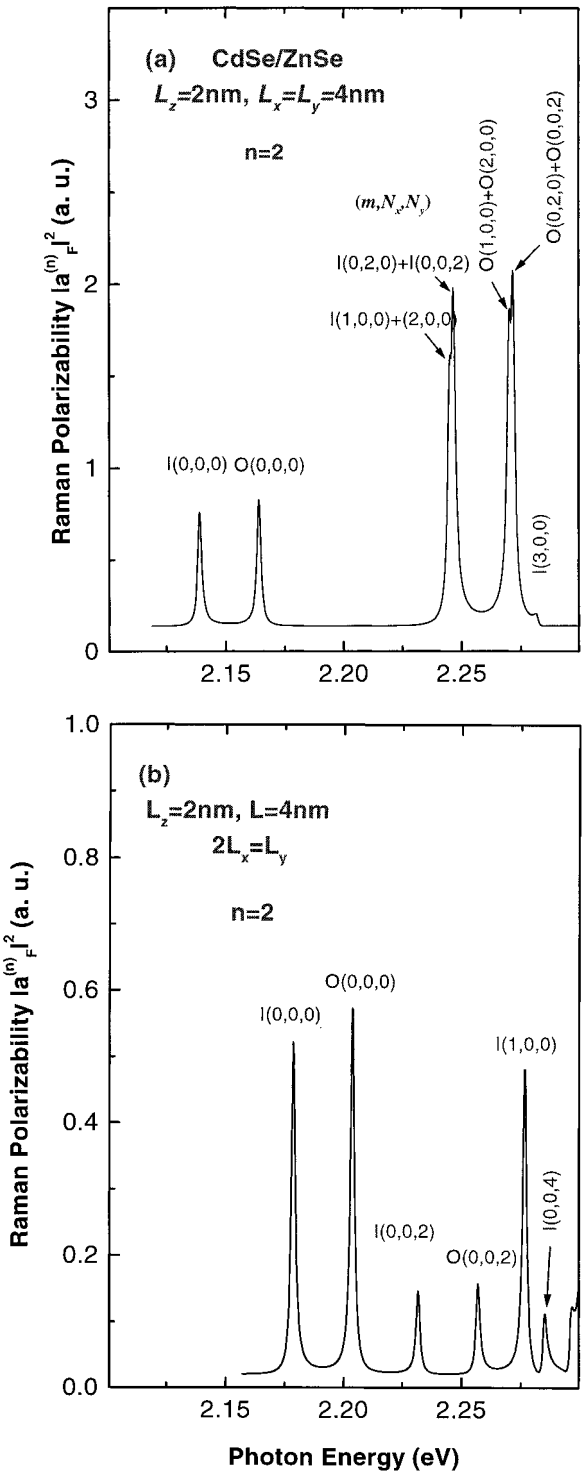

Fig. 1. Raman polarizability $|a_F^{(n)}|^2$, given by Eq. (3) as a function of laser energy for CdSe dots in ZnSe. The figures correspond to the $n = 2$ LO-optical confined mode of CdSe. a) Symmetric case where $L_z = 2$ nm and $L_x = L_y = 4$ nm. b) Asymmetric QD with $L_z = 2$ nm, $L = \sqrt{L_x L_y} = 4$ nm and $2L_x = L_y$

a function of the laser energy for a CdSe SAQD in ZnSe. The values used for the CdSe(ZnSe) calculations are $m_e = 0.112(0.16)\, m_0$, $m_{hz} = 1.2(0.38)\, m_0$, $m_{hxy} = 0.45 m_0$, $E_g = 1.84(2.82)$ eV, $\Delta_c = 0.4 E_g$, $\epsilon_0 = 9.3$, $\beta_L = 1.576 \times 10^{-6}$, $\omega_L = 209.0\,\mathrm{cm}^{-1}$. In the figure, all excitonic transitions correspond to $n_e = n_h = 1$ subbands and the incoming and outgoing resonance peaks are labeled by $\mathrm{I}(m, N_x, N_y)$ and $\mathrm{O}(m, N_x, N_y)$, respectively. Fig. 1a presents $|a_F^{(n)}|^2$ for SAQDs with circular cross section, while the non-symmetric case is shown in Fig. 1b. In both cases $L_z = 2$ nm and $L = \sqrt{L_x L_y} = 4$ nm but in Fig. 1b $2L_x = L_y$. From the figures it is clearly seen that degeneracy present in the circular symmetry case is broken for the elliptical cross-section one, and additional features appear in between the peaks that correspond to the first ($m = 0$) and second ($m = 1$) internal exciton motion states. The difference in energy between $\mathrm{I}(0,0,0)$ and $\mathrm{I}(0,0,2)$ in the Raman intensity spectrum of Fig.1b is proportional to $\hbar\omega_y$ or equivalently to L_y^{-2}. The same is achieved for the outgoing resonant peaks or similar features of the Raman spectrum.

In summary, the resonant Raman scattering intensity for anisotropic QDs has been calculated. The splittings of the excitonic center-of-mass quantum numbers observed in the scattering intensity reflect the quantum dot geometry proving that the resonant Raman technique is a suitable method to characterize the SAQDs. Direct comparison with experimental data would yield important structural information.

SEU acknowledges support from US DOE grant DE-FG02-91ER45334.

References

[1] P.M. Petroff and G. Medeiros-Ribeiro, MRS Bull. **21**, 50 (1996).
[2] M. Fricke, A. Lorke, J.P. Kotthaus, G. Medeiros-Ribeiro, and P.M. Petroff, Europhys. Lett. **36**, 197 (1996).
[3] M. Grundmann et al., Phys. Rev. Lett. **74**, 4043 (1995).
[4] A. Cantarero, C. Trallero-Giner, and M. Cardona, Phys. Rev. B **39**, 8388 (1989).
[5] R.J. Elliot, Phys. Rev. **108**, 1384 (1957).
[6] A.K. Sood, J. Menendez, M. Cardona, and K. Ploog, Phys. Rev. Lett. **54**, 2111 (1985).
[7] C. Trallero-Giner and F. Comas, Phys. Rev. B **37**, 4583 (1988).
[8] J. Song and S.E. Ulloa, Phys. Rev. B **52**, 9015 (1995).
[9] E. Menéndez-Proupin, C. Trallero-Giner, and S.E. Ulloa, to be published.
[10] M. Strassburg, V. Kutzer, U.W. Pohl, A. Hoffmann, I. Broser, N.N. Ledentsov, D. Bimberg, A. Rosenauer, U. Fischer, D. Gerthsen, I.L. Krestnikov, M.V. Maximov, P.S. Kopev, and Zh.I. Alferov, Appl. Phys. Lett. **72**, 942 (1998).
[11] M.Y. Shen, T. Goto, E. Kurts, Z. Zhu, and T. Yao, J. Phys.: Condensed Matter **10**, L171 (1998).